Supplementary Information

Relations between compression and thermal contraction in 1,2,4-trichlorobenzene and melting of trichlorobenzene isomers

Maciej Bujak[a,*], Marcin Podsiadło[b] and Andrzej Katrusiak[b,*]

[a]*Faculty of Chemistry, University of Opole, Oleska 48, 45-052 Opole, Poland; *E-mail: mbujak@uni.opole.pl;*
Tel: +48(77)452-7159; [b]*Faculty of Chemistry, Adam Mickiewicz University, Umultowska 89b, 61-614 Poznań, Poland;*
**E-mail: katran@amu.edu.pl; Tel: +48(61)829-1590*

Experimental

In-situ low-temperature and high-pressure crystal growth

The commercially available 1,2,4-trichlorobenzene (99%, purum, Acros Organics), distilled at reduced pressure, was used for the low-temperature and high-pressure single-crystal X-ray diffraction and compressibility measurements. It was isobarically frozen in a glass capillary (the internal diameter of 0.3 mm and the wall 0.01 mm thick). The liquid sample, filling *ca.* 0.5 mm of the sealed capillary, was cooled in a nitrogen gas stream from an Oxford Cryosystems attachment. At *ca.* 250 K the 124TCB sample froze as a polycrystalline material, which then was warmed to *ca.* 283 K, and the single crystal was grown by temperature cycling, at a rate of 1-2 K·min^{-1}, close to the melting point of 290.07 K [D. R. Lide, ed., *CRC Handbook of Chemistry and Physics*, Internet Version 2007, (87th Edition), Taylor and Francis, Boca Raton, FL, 2007]. This gradually reduced the number of crystal grains left in each cycle (Figure S1). The single-crystal X-ray intensity data were collected at 270.0(1) K, and then the same crystal sample was cooled down and the diffraction data at 100.0(1) K were measured.

A modified Merrill-Bassett diamond-anvil cell, DAC [L. Merrill, W. A. Bassett, *Rev. Sci. Instrum.*, 1974, **45**, 290–294; W. A. Bassett, *High Press. Res.*, 2009, **29**, 163–186] was used for the high-pressure freezing of 124TCB. A general experimental procedure for the high-pressure crystallization was previously reported (Figure S2, [R. Fourme, *J. Appl. Crystallogr.* 1968, **1**, 23–30; W. L. Vos, L. W. Finger, R. J. Hemley, H. Mao, *Phys. Rev. Lett.* 1993, **71**, 3150–3153; D. R. Allan, S. J. Clark, M. J. P. Brugmans, G. J. Ackland, W. L. Vos, *Phys. Rev. B, Condens. Mat.* 1998, **58**, R11809–R11812; M. Bujak, A. Budzianowski, A. Katrusiak, *Z. Kristallogr.* 2004, **219**, 573–579]). The diameter of the diamond culets was 0.8 mm. The gasket was made of 0.3 mm thick steel foil, with a 0.50 mm in diameter hole, spark-eroded and pre-indented to *ca.* 0.36 mm [A. Katrusiak, *J. Appl. Crystallogr.* 1999, **32**, 1021–1023]. The first data set was collected at 0.16(5) GPa. Then the pressure was increased and the new single crystal of 124TCB was grown. The second data set was collected at 0.64(5) GPa in an analogous way. The ruby-fluorescence method, using a BETSA PRL spectrometer, was utilized to measure the pressure in the DAC [J. D. Barnett, S. Block, G. J. Piermarini, *Rev. Sci. Instrum.* 1973, **44**, 1–9; G. J. Piermarini, S. Block, J. D. Barnett, R. A. Forman, *J. Appl. Phys.* 1975, **46**, 2774–2780] with the accuracy of 0.05 GPa.

Data collection, data reduction, structure solution and refinement

The low-temperature ambient-pressure (0.1 MPa) and room-temperature (295 K) high-pressure diffraction data were collected on Xcalibur Eos and KUMA KM4-CCD diffractometers, respectively, both with the graphite-monochromated Mo$K\alpha$ radiation. At 270.0(1) and 100.0(1) K the reflections were measured using the 10 s exposure time and ω-scan technique with $\Delta\omega = 1$ and 0.75°, respectively. The pressure-frozen single crystals of 124TCB were centred on a diffractometer using the shadow method [A. Budzianowski, A. Katrusiak, in *High-Pressure Crystallography,* eds. A. Katrusiak, P. F. McMillan, Dordrecht: Kluwer Academic Publishers, 2004, pp. 101–112]. The room-temperature high-pressure intensity data, at 0.16(5) and 0.64(5) GPa, were collected using the φ- and ω-scan techniques with $\Delta\omega/\Delta\varphi = 0.75°$ and 50 s and 29 s exposures, respectively. All data were accounted for the Lorentz, polarization and sample absorption effects [Agilent Technologies, 2010, *CrysAlis Pro, version 171.35.4*] and the high-pressure data additionally for the absorption of X-rays by the DAC and shadowing of the single crystal by the gasket edges [A. Katrusiak, *REDSHABS*, 2003, *Program for correcting reflections intensities for DAC absorption, gasket shadowing and the sample-crystal absorption.* Adam Mickiewicz University, Poznań, Poland; A. Katrusiak, *Z. Kristallogr.* 2004, **219**, 461–467]. The structures were solved by direct methods and refined with *SHELX-97* [G. M. Sheldrick, *Acta Crystallogr.* 2008, **A64**, 112–122]. The Cl atoms were refined with anisotropic displacement parameters. The C atoms were refined with anisotropic displacement parameters in the low-temperature and isotropically in the high-pressure structures. The H atoms were located in subsequent difference Fourier maps and isotropically refined using the riding model with constrained C–H distances and U_{eq}'s equal to 1.2 times U_{eq}'s of the corresponding C atoms. The *CrysAlis CCD* and *CrysAlis Pro* programs [Oxford Diffraction, 2009, *CrysAlis CCD, version 1.171.33.36d*; Agilent Technologies, 2010, *CrysAlis Pro, version 171.35.4*] were used for the data collection, unit-cell refinement and data reductions (initial reduction of the high-pressure intensity data). The 124TCB crystal data and structure determination summary are listed in Table S1. The bond lengths, angles and the shortest intra- and intermolecular distances are presented in Tables S2 and S3. The compressed intermolecular contacts have been compared using the Hirshfeld-surface analyses together with the two-dimensional fingerprint plots, provided by *Crystal Explorer* [S. K. Wolff, D. J. Grimwood, J. J. McKinnon, D. Jayatilaka, M. A. Spackman, 2007, *CrystalExplorer 2.0* (r 313). University of Western Australia; J. J. McKinnon, M. A. Spackman, A. S. Mitchell, *Acta Crystallogr.* 2004, **B60**, 627–668; M. A. Spackman, J. J. McKinnon, D. Jayatilaka, *CrystEngComm* 2008, **10** 377–388; M. A. Spackman, D. Jayatilaka, *CrystEngComm* 2009, **11** 19–32]. The structure drawings were prepared using *Mercury* [C. F. Macrae,

I. J. Bruno, J. A. Chisholm, P. R. Edgington, P. McCabe, E. Pidcock, L. Rodriguez-Monge, R. Taylor, J. van de Streek, P. A. Wood, *J. Appl. Cryst.* 2008, **41** 466–470].

Compressibility measurement

The room-temperature, at 295(2) K, compressibility measurement, between ambient pressure and 1 GPa, was performed in the piston-and-cylinder apparatus [K. Dziubek, A. Katrusiak, *Z. Kristallogr.* 2014, **229**, 129−134]. The pressure was increased in *ca.* 20 MPa steps.

Results and discussion

The aromatic rings are essentially planar, with the maximum deviation of the C-atoms from this plane of 0.016(4) Å at 270 K/0.1 MPa. The Cl-atoms do not deviate significantly from the planes defined by the C-atoms. The maximum deviation of 0.090(19) Å was found for the Cl14 atom at 295 K/0.64 GPa. The principal geometrical features of the 124TCB molecules remain, within the limit of 3 esd's, essentially constant at both studied temperatures and are, in general, regular for the aromatic C–C, and C–Cl and C–H bonds and corresponding valence and torsion angles (Table S2). The bond distances and valence angles are also comparable with the previous results obtained by means of electron diffraction [R. Schoppe, *Z. Phys. Chem. (Leipzig)* 1936, **34**, 461–470] and similar to those observed in benzene and its chloro derivatives [A. Budzianowski, A. Katrusiak, *Acta Crystallogr.* 2006, **B62**, 94–101; D. Andre, R. Fourme, M. Renaud, *Acta Crystallogr.* 1971, **B27**, 2371–2380; R. Boese, M. T. Kirchner, J. D. Dunitz, G. Filippini, A. Gavezzotti, *Helv. Chim. Acta* 2001, **84**, 1561–1577; M. Bujak, K. Dziubek, A. Katrusiak, *Acta Crystallogr.* 2007, **B63**, 124–131]. They are also in agreement with the values found in the other crystals that contain 124TCB molecules [*e.g.* J. W. Buchler, A. De Cian, J. Fischer, M. Kihn-Botulinski, H. Paulus, R. Weiss, *J. Am. Chem. Soc.* 1986, **108**, 3652–3659].

The intramolecular Cl···Cl distances between vicinal Cl11 (Cl21) and Cl12 (Cl22) chlorines, with the shortest 3.155(3) Å at 270 K/0.1 MPa, are shorter than the sum of van der Waals radii for those atoms (Table S3) [A. Bondi, *J. Phys. Chem.* 1964, **68**, 441–451] and thus indicative of a certain amount of steric crowding. The data show that this crowding is relieved rather through the changes of Cl–C–C angles, than the Cl–C and C–C bonds elongation. At both temperatures the Cl11–C11–C12 (Cl21–C21–C22) and Cl12–C12–C11 (Cl22–C22–C21) angles are larger than 120º (average 121.2º at 100 K/0.1 MPa) whereas, the adjacent Cl11–C11–C16 (and C21–C21–C16) and Cl12–C12–C13 (and Cl22–C22–C23) angles are compressed to 118.7º on average at 100 K/0.1 MPa (Table S2). The remaining Cl–C–C angles are equal within the experimental limits. Circling the ring, the endocyclic C–C–C angles (120º on average) show small alternations with the largest difference of 4.6(7)º at 270 K/0.1 MPa. Such differences are comparable to those found in the low-temperature structure of 123TCB isomer where the steric effects of chlorines are more prominent [A. J. Blake, R. Blom, S. Cradock, S. L. Davidson, D. W. H. Rankin, *J. Mol. Struct.* 1990, **240**, 95–110].

Decreasing temperature and increasing pressure, in general, decreases intermolecular distances, and increases density which affects the Hirshfeld surfaces and the fingerprint plots (Figures S4 and S5). The observation that more of the intermolecular contacts are formed at lower temperatures and higher pressures is consistent with results observed in other studies on chloro- compounds [*e.g.* M. Bujak, M. Podsiadło, A. Katrusiak, *J. Phys. Chem. B* 2008, **112**, 1184–1188].

The fingerprint plots illustrate that intermolecular contacts for two symmetry-independent 124TCB molecules are somewhat different, especially in the case of H···H interactions, that are almost absent for the second (C21-C26) molecule. On decreasing temperature and increasing pressure the fingerprint plots look much the same, since no drastic structural changes, *e.g.* a change associated with a phase transition, is encountered over the studied temperature and pressure range. The finding that increasing density is observed manifests itself in the progressive slightly compact plots and their movement to lower d_e and d_i values on decreasing temperature and increasing pressure. Furthermore, as referred above, the increasing importance of the Cl···Cl and Cl···H interactions, at low temperature and at high pressure is particularly apparent - these two types of interactions becoming more prominent at 100 K/0.1 MPa and 295 K/0.64 GPa.

All the Cl···Cl and Cl···H intermolecular contacts are important for the packing mode and molecular association in the crystals and suggest that specific interactions exist between 124TCB molecules. Those contacts could be classified as type II and somewhat distorted type II interaction (θ_1 and θ_2 angles are not so far from 90 and 180° (Table S3; [G. R. Desiraju, R. Parthasarathy, *J. Am. Chem. Soc.* 1989, **111**, 8725–8726; V. R. Pedireddi, D. S. Reddy, B. S. Goud, D. C. Craig, A. D. Rae, G. R. Desiraju, *J. Chem. Soc. Perkin Trans 2* 1994, 2353–2360; L. Brammer, E. A. Bruton, P. Sherwood, *Cryst. Growth Des.* 2001, **1**, 277–290; M. Fourmigué, *Curr. Opin. Solid State Mater. Sci.* 2009, **13**, 36–45; F. F. Awwadi, R. D. Willett, K. A. Peterson, B. Twamley, *Chem. Eur. J.* 2006, **12**, 8952–8960]).

It is characteristic that the Cl···H contacts are compressed more than contacts Cl···Cl (Figure 7). The same trend, but at a smaller rate is observed on reducing temperature. Most interestingly, the shortest Cl21···Cl24^{III} contact in 124TCB increases from 3.499(2) Å at 270 K/0.1 MPa to 3.539(13) Å at 295 K/0.16 GPa; and from 3.423(1) Å at 100 K/0.1 MPa to 3.440(17) Å and 295 K/0.64 GPa. This can be an indication of decreasing importance of Cl21···Cl24 interactions with pressure, which is consistent with the recently observed replacement of Br···Br contacts by contacts C–H···Br in high-pressure phase of CH_3Br [M. Podsiadło, A. Olejniczak, A. Katrusiak, *CrystEngComm.* 2014, **16**, 8279−8285]. The C–H···Cl contacts in 124TCB behave differently. The shortest Cl21···H25^{VI} distance of 3.002 Å at 270 K/0.1 MPa increases to 3.132 Å at 295 K/0.16 GPa, however it is practically identical at 100 K/0.1 MPa and 295 K/0.64 GPa, of 2.960 Å and 2.959 Å, respectively. Thus the Cl···Cl and H···Cl contacts are pressure and temperature dependent at a different rate, and pressure differentiates the contacts more pronouncedly than temperature (Figure 7).

Since all the trichlorobenzene isomers form ordered crystals built form molecules that do not show the conformational freedom, the differences in their properties are mainly related to the enthalpy component [A. Gavezzotti, *J. Chem. Soc., Perkin Trans. 2* 1995, 1399–1404] and could be explained by the shape/symmetry of molecules and different-packing efficiency, which in turn, depends on the formed intermolecular interactions. All these mentioned factors are more favourable for the highest-melting highest-symmetrical 135TCB: (i) the electronegative chlorine atoms are in the perfect geometrical positions – they are bonded to every second carbon atom; (ii) owing to the distant location the chlorine atoms do not interfere with each other and the sterical hindrances are minimized; (iii) the 1,3,5-location of substituents requires slightly more space for each molecule, but at the same time it secures a free access to the chlorine atoms increasing the possibility of potential intermolecular interactions.

The differences in molecular packing patterns and intermolecular interactions between the trichlorobenzene isomers are presented on the two-dimensional fingerprint plots (Figure S5). The area coverage and the density of points on the fingerprint plots facilitate the analysis of the specific types of interactions and confirms that 124TCB molecules, in general, are engaged in less interactions (absence of H···H in one of two symmetry-independent molecules), which is additionally reflected in the lowest packing coefficient (Table 2). The highest melting point of 135TCB corresponds well to the Cl···Cl interactions being more pronounced in that structure than in two other isomers.

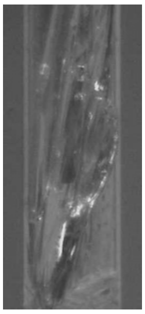

Figure S1. The isobarically frozen, in a glass capillary, 124TCB at 270 K/0.1 MPa.

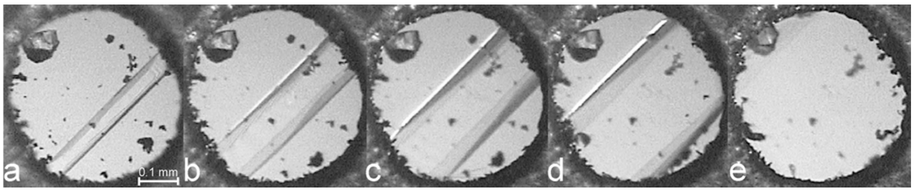

Figure S2. Stages of isochoric growth of the 124TCB single crystal in a diamond-anvil cell leading to the sample fully filling the high-pressure chamber (0.42 mm in diameter) at 295 K/0.16 GPa. The small ruby chip, for pressure calibration, is located at the top edge of the high-pressure chamber.

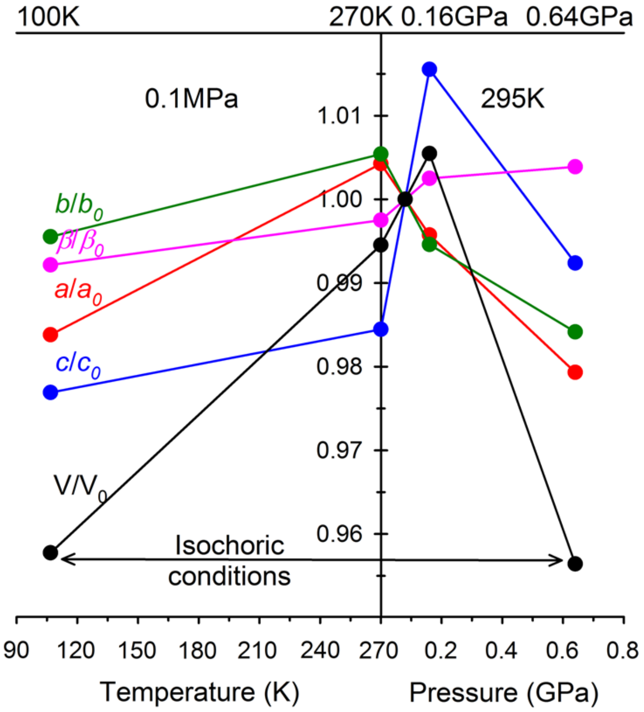

Figure S3. Relative changes in unit-cell parameters of 124TCB at isobaric (left), pseudo-isochoric (center) and isothermal (right) transformations region. The parameters have been related to the average dimensions between 270 K/0.1 MPa and 295 K/0.16 GPa.

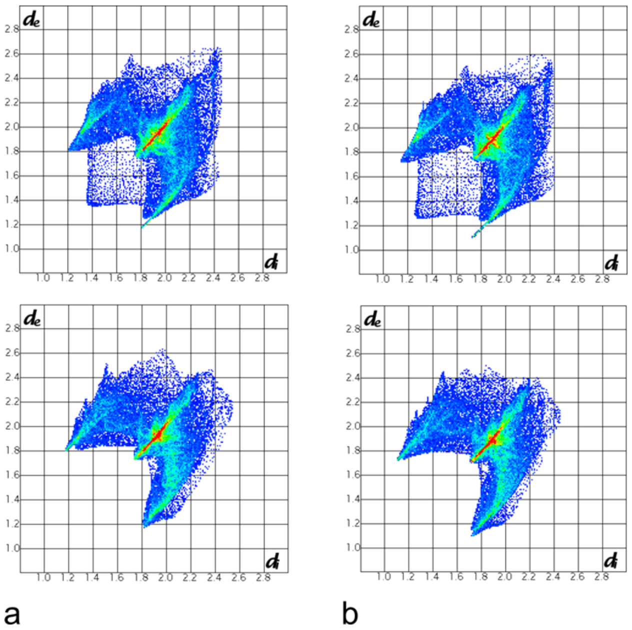

Figure S4. The two-dimensional fingerprint plots for two symmetry-independent trichlorobenzene molecules (the upper plot corresponds to the first C11-C16 molecule, whereas the lower one to the second C21-C26 molecule) in the high-pressure structures of 124TCB at: (a) 295 K/0.16 GPa and (b) 295 K/0.64 GPa.

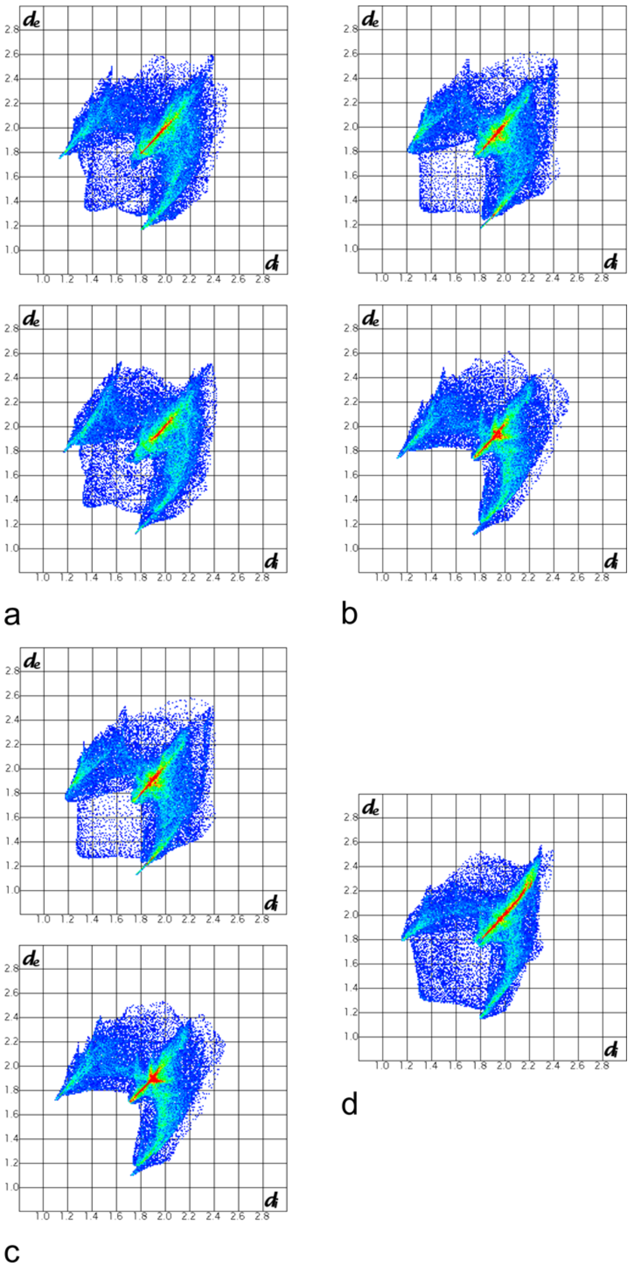

Figure S5. Two-dimensional fingerprint plots for the ambient-pressure structures of: (a) 123TCB at 298 K (the upper plot corresponds to the first C1-C11 molecule, whereas the lower one to the second C2-C12 symmetry-independent molecule); (b), (c) 124TCB at 270 and 100 K (the upper plot corresponds to the first C11-C16 molecule, whereas the lower one to the second C21-C26 symmetry-independent molecule), and (d) 135TCB at 293 K, respectively.

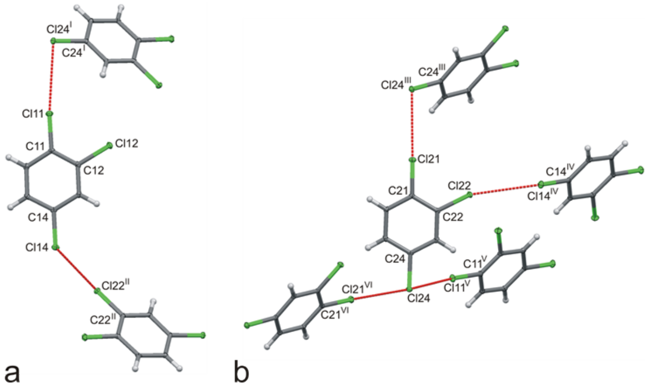

Figure S6. The intermolecular Cl···Cl contacts in the low-temperature structure of 124TCB at 100 K/0.1 MPa, denoted by the red lines, formed by two symmetry-independent 124TCB molecules. Displacement ellipsoids are plotted at the 25% probability level. Symmetry codes: (I) $3/2 - x$, $-1/2 + y$, $1/2 - z$; (II) $1/2 + x$, $1/2 - y$, $1/2 + z$; (III) $1/2 + x$, $1/2 - y$, $-1/2 + z$; (IV) $-1/2 + x$, $1/2 - y$, $-1/2 + z$; (V) $3/2 - x$, $1/2 + y$, $1/2 - z$; (VI) $-1/2 + x$, $1/2 - y$, $1/2 + z$.

Table S1. The 124TCB crystal data and structure determination summary.

temperature	270.0(1) K	100.0(1) K	295(2) K	295(2) K
pressure	0.1 MPa	0.1 MPa	0.16(5) GPa	0.64(5) GPa
formula	$C_6H_3Cl_3$	$C_6H_3Cl_3$	$C_6H_3Cl_3$	$C_6H_3Cl_3$
fw, g/mol	181.43	181.43	181.43	181.43
crystal size, mm	0.3 x 0.1 x 0.1	0.3 x 0.1 x 0.1	0.42 x 0.42 x 0.24	0.40 x 0.40 x 0.24
crystal system	monoclinic	monoclinic	monoclinic	monoclinic
space group	$P2_1/n$	$P2_1/n$	$P2_1/n$	$P2_1/n$
Z, Z'	8, 2	8, 2	8, 2	8, 2
a, Å	3.8788(5)	3.7998(4)	3.8459(5)	3.7825(7)
b, Å	26.948(3)	26.683(3)	26.658(3)	26.378(3)
c, Å	13.6006(13)	13.4964(13)	14.03(4)	13.71(4)
β, °	93.164(9)	92.665(9)	93.63(5)	93.76(6)
V, Å^3	1419.5(3)	1366.9(2)	1436(4)	1365(4)
ρ, g/cm^3	1.698	1.763	1.678	1.766
μ, mm^{-1}	1.186	1.232	1.173	1.234
θ range, °	3.00 – 25.00	3.02 – 25.00	3.06 – 24.91	3.09 – 24.94
index ranges	$-4 \leq h \leq 4$	$-4 \leq h \leq 4$	$-4 \leq h \leq 4$	$-4 \leq h \leq 4$
	$-32 \leq k \leq 32$	$-31 \leq k \leq 31$	$-31 \leq k \leq 31$	$-31 \leq k \leq 31$
	$-16 \leq l \leq 16$	$-15 \leq l \leq 16$	$-3 \leq l \leq 3$	$-3 \leq l \leq 3$
reflns collected	28754	10317	7085	6941
R_{int}	0.1340	0.0581	0.1144	0.1388
data [$I > 2\sigma(I)$]	1793	2053	404	434
data/parameters	2503/163	2419/163	540/103	528/103
GOF on F^2	1.091	1.131	1.134	1.446
R_1 [$I > 2\sigma(I)$]	0.0756	0.0428	0.0601	0.1112
R_1 (all data)^a	0.1023	0.0532	0.0823	0.1279
wR_2 (all data)^a	0.2322	0.1208	0.1895	0.3072
lrgst diff peak, e/Å^3	0.773	0.504	0.266	0.560
lrgst diff hole, e/Å^3	–0.541	–0.451	–0.264	–0.528

$^a R_1 = \Sigma||F_o|-|F_c||/\Sigma|F_o|$; $wR_2 = \{\Sigma[w(F_o^2-F_c^2)^2]/\Sigma[w(F_o^2)^2]\}^{1/2}$; $w = 1/[\sigma^2(F_o^2)+(aP)^2 + bP]$, where $P = (F_o^2 + 2F_c^2)/3$

Table S2. The molecular dimensions (Å, º) of 124TCB at 270 K/0.1 MPa, 100 K/0.1 MPa, 295 K/0.16 GPa and 295 K/0.64 GPa.

Atoms; Temperature/Pressure	270 K/0.1 MPa	100 K/0.1 MPa	295 K/0.16 GPa	295 K/0.64 GPa
Cl11–C11	1.720(6)	1.725(3)	1.78(2)	1.78(3)
Cl12–C12	1.736(6)	1.737(3)	1.745(16)	1.71(2)
Cl14–C14	1.733(6)	1.737(3)	1.74(2)	1.75(3)
C11–C12	1.369(8)	1.383(5)	1.347(16)	1.367(19)
C11–C16	1.393(8)	1.389(5)	1.354(17)	1.36(2)
C12–C13	1.375(8)	1.379(5)	1.350(15)	1.370(19)
C13–C14	1.374(8)	1.383(5)	1.346(13)	1.367(17)
C14–C15	1.376(8)	1.382(5)	1.348(15)	1.365(19)
C15–C16	1.386(8)	1.384(5)	1.349(14)	1.363(18)
Cl21–C21	1.734(6)	1.737(3)	1.68(3)	1.77(5)
Cl22–C22	1.723(5)	1.724(3)	1.76(3)	1.83(5)
Cl24–C24	1.730(5)	1.738(3)	1.79(3)	1.76(3)
C21–C22	1.394(8)	1.390(5)	1.368(14)	1.355(16)
C21–C26	1.367(7)	1.379(5)	1.45(5)	1.46(7)
C22–C23	1.386(8)	1.396(5)	1.374(18)	1.355(17)
C23–C24	1.392(7)	1.385(5)	1.372(19)	1.354(17)
C24–C25	1.363(8)	1.379(5)	1.371(13)	1.357(16)
C25–C26	1.398(8)	1.389(5)	1.372(19)	1.355(17)
Cl11–C11–C12	122.3(5)	121.3(3)	123.9(10)	121.6(11)
Cl11–C11–C16	118.6(4)	119.2(3)	119.7(19)	116(2)
Cl12–C12–C11	120.0(5)	120.6(3)	121.8(11)	122.0(13)
Cl12–C12–C13	119.3(4)	118.7(3)	116.6(15)	119.6(18)
Cl14–C14–C13	119.0(4)	118.9(3)	121.0(18)	118(2)
Cl14–C14–C15	119.5(5)	119.6(3)	120.6(8)	120.8(10)
C11–C12–C13	120.7(5)	120.6(3)	121.5(15)	117.9(18)
C11–C16–C15	120.9(5)	120.6(3)	123(2)	119(3)
C12–C11–C16	119.1(5)	119.5(3)	116.3(17)	122(2)
C12–C13–C14	119.6(5)	119.1(3)	121(2)	120(3)
C13–C14–C15	121.5(5)	121.5(3)	118.3(17)	121(2)
C14–C15–C16	118.2(5)	118.7(3)	119.6(15)	119.4(18)
Cl21–C21–C22	120.9(4)	120.7(3)	126(3)	122(4)
Cl21–C21–C26	119.0(4)	118.4(3)	120.7(9)	121.9(11)
Cl22–C22–C21	121.8(4)	122.2(3)	117(3)	119(4)
Cl22–C22–C23	117.9(4)	118.3(3)	120.1(12)	119.2(12)
Cl24–C24–C23	118.1(4)	118.7(3)	121.9(8)	118.5(11)
Cl24–C24–C25	119.4(4)	119.1(3)	116.2(19)	117(2)
C21–C22–C23	120.4(5)	119.6(3)	123(3)	122(4)
C21–C26–C25	120.5(5)	120.0(3)	125.4(13)	121.9(17)
C22–C21–C26	120.1(5)	120.9(3)	113(3)	116(4)
C22–C23–C24	117.9(5)	118.5(3)	120.7(15)	119.1(17)
C23–C24–C25	122.5(5)	122.2(3)	121.7(17)	124(2)
C24–C25–C26	118.5(5)	118.8(3)	116.0(19)	116(2)
Cl11–C11–C12–Cl12	–0.9(7)	–2.9(4)	–5.9(17)	–11.1(16)
Cl11–C11–C12–C13	179.8(4)	178.8(3)	177.2(7)	177.1(9)
Cl11–C11–C16–C15	–179.7(5)	–178.9(3)	–177.2(9)	–177.1(9)
Cl12–C12–C13–C14	–178.9(4)	–178.2(2)	–178.4(8)	–178.8(9)
Cl14–C14–C15–C16	–178.6(4)	–178.9(2)	–177.0(7)	–177.7(9)
C11–C12–C13–C14	0.4(9)	0.1(5)	–1.4(16)	–6.7(16)
C12–C11–C16–C15	2.1(8)	0.3(5)	–1.1(16)	–6.8(16)
C12–C13–C14–Cl14	178.6(4)	178.8(3)	177.2(8)	178.5(9)
C12–C13–C14–C15	1.4(9)	0.4(5)	1.2(15)	5.8(17)
C13–C14–C15–C16	–1.4(9)	–0.5(5)	–1.0(17)	–5.2(19)
C14–C15–C16–C11	–0.4(9)	0.2(5)	1.0(16)	5.6(18)
C16–C11–C12–Cl12	177.2(4)	177.9(3)	178.2(6)	179.1(10)
C16–C11–C12–C13	–2.1(8)	–0.4(5)	1.3(17)	7.3(17)
Cl21–C21–C22–Cl22	0.6(7)	0.1(4)	0.2(16)	2.2(19)
Cl21–C21–C22–C23	–179.1(4)	179.9(2)	179.4(9)	–178.8(10)
Cl21–C21–C26–C25	179.6(5)	–179.3(3)	–179.0(7)	–179.6(10)
Cl22–C22–C23–C24	178.5(4)	179.1(2)	–179.6(10)	–179.8(12)
Cl24–C24–C25–C26	178.4(4)	178.8(2)	178.2(7)	179.3(10)
C21–C22–C23–C24	–1.8(8)	–0.7(5)	1.2(17)	1(2)
C22–C21–C26–C25	0.4(8)	1.1(5)	1.1(18)	4(2)
C22–C23–C24–Cl24	–177.9(4)	–178.1(2)	–177.7(7)	–177.8(9)
C22–C23–C24–C25	3.2(8)	1.2(5)	–2.0(16)	–2(2)
C23–C24–C25–C26	–2.8(8)	–0.5(5)	2.2(14)	3.0(19)
C24–C25–C26–C21	0.9(8)	–0.6(5)	–1.8(16)	–4.2(18)
C26–C21–C22–Cl22	179.8(4)	179.8(2)	180.0(10)	178.7(13)
C26–C21–C22–C23	0.0(8)	–0.4(5)	–0.7(18)	–2(2)

Table S3. The geometries (Å, º) of the shortest intra- and intermolecular contacts of 124TCB at 270 K/0.1 MPa, 100 K/0.1 MPa, 295 K/0.16 GPa and 295 K/0.64 GPa.

Atoms; Temperature/Pressure	270 K/0.1 MPa	100 K/0.1 MPa	295 K/0.16 GPa	295 K/0.64 GPa
Cl11···Cl12	3.155(3)	3.167(1)	3.264(22)	3.220(28)
C11–Cl11···Cl12	58.6(2)	59.0(1)	56.1(8)	56.7(9)
Cl11···Cl12–C12	59.1(2)	59.0(1)	58.0(8)	59(1)
C11–Cl11···Cl12–C12	–0.4(3)	–1.3(2)	–2.5(7)	–4.7(6)
Cl12···Cl11	3.155(3)	3.167(1)	3.264(22)	3.220(28)
C12–Cl12···Cl11	59.1(2)	59.0(1)	58.0(8)	59(1)
Cl12···Cl11–C11	58.6(2)	59.0(1)	56.1(8)	56.7(9)
C12–Cl12···Cl11–C11	–0.4(3)	–1.3(2)	–2.5(7)	–4.7(6)
Cl21···Cl22	3.192(2)	3.196(1)	3.159(6)	3.171(7)
C21–Cl21···Cl22	58.7(2)	58.7(1)	58(1)	60(1)
Cl21···Cl22–C22	58.7(2)	58.4(1)	59.1(5)	59.5(6)
C21–Cl21···Cl22–C22	0.3(3)	0.1(2)	0.1(7)	0.9(8)
Cl22···Cl21	3.192(2)	3.196(1)	3.159(6)	3.171(7)
C22–Cl22···Cl21	58.7(2)	58.4(1)	59.1(5)	59.5(6)
Cl22···Cl21–C21	58.7(2)	58.7(1)	58(1)	60(1)
C22–Cl22···Cl21–C21	0.3(3)	0.1(2)	0.1(7)	0.9(8)
Cl11···Cl24$^{\mathrm{I}}$	3.541(2)	3.461(1)	3.547(11)	3.486(16)
C11–Cl11···Cl24$^{\mathrm{I}}$	166.0(2)	166.9(1)	166.4(7)	167.5(7)
Cl11···Cl24$^{\mathrm{I}}$–C24$^{\mathrm{I}}$	88.1(2)	86.9(1)	84.7(6)	86.0(8)
C11–Cl11···Cl24$^{\mathrm{I}}$–C24$^{\mathrm{I}}$	85.2(9)	89.2(6)	76(3)	77(4)
Cl24···Cl11$^{\mathrm{II}}$	3.541(2)	3.461(1)	3.547(11)	3.486(16)
C24–Cl24···Cl11$^{\mathrm{II}}$	88.1(2)	86.9(1)	84.7(6)	86.0(8)
Cl24···Cl11$^{\mathrm{II}}$–C11$^{\mathrm{II}}$	166.0(2)	166.9(1)	166.4(7)	167.5(7)
C24–Cl24···Cl11$^{\mathrm{II}}$–C11$^{\mathrm{II}}$	85.2(9)	89.2(6)	76(3)	77(4)
Cl21···Cl24$^{\mathrm{III}}$	3.499(2)	3.423(1)	3.539(13)	3.440(17)
C21–Cl21···Cl24$^{\mathrm{III}}$	177.6(2)	177.9(1)	177.9(5)	176.1(8)
Cl21···Cl24$^{\mathrm{III}}$–C24$^{\mathrm{III}}$	95.0(2)	94.8(1)	99.0(6)	95.6(8)
C21–Cl21···Cl24$^{\mathrm{III}}$–C24$^{\mathrm{III}}$	159(5)	157(3)	94(30)	145(17)
Cl24···Cl21$^{\mathrm{IV}}$	3.499(2)	3.423(1)	3.539(13)	3.440(17)
C24–Cl24···Cl21$^{\mathrm{IV}}$	95.0(2)	94.8(1)	99.0(6)	95.6(8)
Cl24···Cl21$^{\mathrm{IV}}$–C21$^{\mathrm{IV}}$	177.6(2)	177.9(1)	177.9(5)	176.1(8)
C24–Cl24···Cl21$^{\mathrm{IV}}$–C21$^{\mathrm{IV}}$	–159(5)	–157(3)	–94(30)	–145(17)
Cl14···Cl22$^{\mathrm{V}}$	3.576(2)	3.499(1)	3.624(16)	3.532(18)
C14–Cl14···Cl22$^{\mathrm{V}}$	126.0(2)	126.8(1)	126.2(5)	126.3(6)
Cl14···Cl22$^{\mathrm{V}}$–C22$^{\mathrm{V}}$	158.3(2)	158.9(1)	158.6(7)	158.2(8)
C14–Cl14···Cl22$^{\mathrm{V}}$–C22$^{\mathrm{V}}$	–122.2(6)	–119.2(4)	–123(1)	–122(1)
Cl22···Cl14$^{\mathrm{VI}}$	3.576(2)	3.499(1)	3.624(16)	3.532(18)
C22···Cl22–Cl14$^{\mathrm{VI}}$	158.3(2)	158.9(1)	158.6(7)	158.2(8)
Cl22···Cl14$^{\mathrm{VI}}$–C14$^{\mathrm{VI}}$	126.0(2)	126.8(1)	126.2(5)	126.3(6)
C22–Cl22···Cl14$^{\mathrm{VI}}$–C14$^{\mathrm{VI}}$	122.2(6)	119.2(4)	123(1)	122(1)
Cl24···H16$^{\mathrm{IV}}$	3.095	2.998	3.150	2.959
C24–Cl24···H16$^{\mathrm{IV}}$	154.4	153.8	156.1	156.8
Cl24···H16$^{\mathrm{IV}}$–C16$^{\mathrm{IV}}$	114.8	114.7	119.9	119.8
C24–Cl24···H16$^{\mathrm{IV}}$–C16$^{\mathrm{IV}}$	151.1	152.9	153.7	149.1
H16···Cl24$^{\mathrm{III}}$	3.095	2.998	3.150	2.959
C16–H16···Cl24$^{\mathrm{III}}$	114.8	114.7	119.9	119.8
H16···Cl24$^{\mathrm{III}}$–C24$^{\mathrm{III}}$	154.4	153.8	156.1	156.8
C16–H16···Cl24$^{\mathrm{III}}$–C24$^{\mathrm{III}}$	–151.1	–152.9	–153.7	–149.1
Cl21···H25$^{\mathrm{VI}}$	3.002	2.960	3.132	2.959
C21–Cl21···H25$^{\mathrm{VI}}$	113.1	112.3	112.4	111.2
Cl21···H25$^{\mathrm{VI}}$–C25$^{\mathrm{VI}}$	151.9	150.8	149.9	146.2
C21–Cl21···H25$^{\mathrm{VI}}$–C25$^{\mathrm{VI}}$	159.1	159.7	161.9	159.0
H25···Cl21$^{\mathrm{V}}$	3.002	2.960	3.132	2.959
C25–H25···Cl21$^{\mathrm{V}}$	151.9	150.8	149.9	146.2
H25···Cl21$^{\mathrm{V}}$–C21$^{\mathrm{V}}$	113.1	112.3	112.4	111.2
C25–H25···Cl21$^{\mathrm{V}}$–C21$^{\mathrm{V}}$	–159.1	–159.7	–161.9	–159.0

Symmetry codes: (I) 3/2 – *x*, –1/2 + *y*, 1/2 – *z*; (II) 3/2 – *x*, 1/2 + *y*, 1/2 – *z*; (III) 1/2 + *x*, 1/2 – *y*, –1/2 + *z*; (IV) –1/2 + *x*, 1/2 – *y*, 1/2 + *z*; (V) 1/2 + *x*, 1/2 – *y*, 1/2 + *z*; (VI) –1/2 + *x*, 1/2 – *y*, –1/2 + *z*.

Table S4. The void volume calculations of 124TCB (0.5 Probe Radius and 0.5 Approx. Grid Spacing) [C. F. Macrae, I. J. Bruno, J. A. Chisholm, P. R. Edgington, P. McCabe, E. Pidcock, L. Rodriguez-Monge, R. Taylor, J. van de Streek, P. A. Wood, *J. Appl. Cryst.* 2008, **41** 466–470].

Temperature/Pressure	270 K/0.1 MPa	100 K/0.1 MPa	295 K/0.16 GPa	295 K/0.64 GPa
Void volume of the unit cell (Å^3)	74.63	54.14	90.06	52.43
% of the unit cell	5.3	4.0	6.3	3.8